INTEGRATED MODELLING OF CORE AND DIVERTOR PLASMAS FOR DEMO-FNS HYBRID FACILITY

A.Y. DNESTROVSKIY
NRC "Kurchatov Institute"
Moscow, Russian Federation
Email: dnestrovskiy_ay@nrcki.ru

A.S.KUKUSHKIN
NRC "Kurchatov Institute"
National Research Nuclear University MEPhI
Moscow, Russian Federation
Email: ank755@gmail.com

B.V.KUTEEV
NRC "Kurchatov Institute"
National Research Nuclear University MEPhI
Moscow, Russian Federation
Email: kuteev_bv@nrcki.ru

V.Y.SERGEEV
Peter the Great St.Petersburg Polytechnic University
Saint Petersburg, Russian Federation
Email: v.sergeev@spbstu.ru

Abstract

The steady state regime for tokamak based DEMO Fusion Neutron Source (DEMO-FNS) with parameters R/a=3.2 m/1m, B=5T, I_{pl}=4-5 MA, P_{NBI}=30MW and P_{ECR}=6MW is studied using a consistent modeling of the central and divertor plasma. In our formulation, the divertor plasma state is determined by the values of heat flux P_{SOL}, the pressure of the neutrals p_n and the neon content in N_{Ne} the divertor region. As boundary conditions for the central plasma we use values of density and temperatures of ions and electrons on the separatrix, the neon impurity relative density at the separatrix and the neutral flux through the separatrix toward to the central plasma column. In the divertor region all values calculated by the code SOLPS4.3 for a set of operating points (~150 in our case) with different values of P_{SOL}, p_n and N_{Ne}, and then the calculation results are approximated by analytical formulas. Heat transport in the central plasma is calculated using the ASTRA code and sets the scaling for the confinement time of energy IPB(y,2) with variation of *H-factor*. The simplified physical model for the description of the pedestal in H-mode inside the separatrix is used, based on the scalings for width and pressure at the pedestal. The hydrogen (deuterium and tritium) density is modelled taking into account sources of neutrals coming from divertor region, as well as the injection of fast atoms and/or pellet injection. The neon density and radiation in the main plasma is calculated using the STRAHL code. The Helium plasma dilution is taken into account in the main plasma to estimate the maximum permissible helium confinement values.

The simulation determines the operational regime of DEMO-FNS, in which the heat load on divertor plates remain at an acceptable level, and the divertor plasma does not go into "detachment" mode and double-null separatrix configuration is kept to be symmetric. The dependence of these conditions on the impurity level is investigated.

1. INTRODUCTION

This paper reports on the progress towards developing the integrated model of the core, pedestal and SOL plasma in the DEMO Fusion Neutron Source (DEMO-FNS) device currently being designed in RF [1]. We follow the approach developed for ITER [2] where parameterization of the results of a series of calculations of the edge plasma parameters performed with the SOLPS4.3 code suite [3] with broad variation of the input parameters is used to produce the boundary conditions for the transport model of the plasma inside the separatrix. The present DEMO-FNS design differs strongly from ITER (in particular, it employs a double-null divertor configuration); therefore realization of the approach of [2] requires special consideration. The principal aim of the paper is to find out, whether sustainable divertor power loading and required fusion performance can simultaneously be achieved in DEMO-FNS with neon seeding.

2 THE INTEGRATED MODEL

We study the steady-state regime for a neutron source DEMO-FNS [1, 4-6] based on a tokamak conception with parameters R/a=3.2m/1m, B=5T, I_{pl}=4-5MA, using a consistent simulation of central and divertor plasma. The complete model includes the following tasks:

(a) The processes in the central plasma are described by the code ASTRA [7]. The power balance is given by heat conduction equations for ion and electron sources with input power from the beam P_{NB}= 30MW, ECR heating P_{EC}= 6MW, absorbed by electrons, and from the alpha-particles P_{α}. Heat losses include the bremsstrahlung P_{br}, synchrotron P_{sync}, and the impurity neon radiation P_{imp}, so the integral power balance is represented in the form $P_{SOL} = P_{in} - P_{rad}$, where $P_{in} = P_{NB} + P_{EC} + P_{\alpha}$ is the total heating power and $P_{rad} = P_{br} + P_{sync} + P_{imp}$ is the total radiation from the main plasma, P_{SOL} is the heat flux from the main plasma in divertor region. The energy confinement time τ_E is prescribed by the IPB(y,2) scaling with the specified *H-factor*, and the coefficient of thermal conductivity is set radially uniform except for the pedestal zone (see (h) below).

(b) The balance of the main ions (deuterium and tritium) in the main plasma is described by the diffusion equation with sources from the ionization of the neutrals from the divertor volume S_{0sep}, from the beam S_{NB} and by the model external source S_{pel} from the pellet injection and is represented as $S_{sep} = S_{0,\mathrm{sep}} + S_{NB} + S_{pel}$, where S_{sep} is the flow of the main ions from the plasma into the divertor volume. Particle confinement is prescribed to be proportionally to the energy confinement with a variable coefficient $c_p = \tau_p/\tau_E$, where τ_p is the particle confinement time, the particle diffusion coefficient is taken proportional to the heat conductivity coefficient, the fraction of tritium in the main plasma f_T is prescribed. The helium balance in the main plasma is calculated with the helium source from D-T reaction and prescribed helium confinement using the factor $c_{He} = \tau_{He}/\tau_p$, where τ_{He} is the alpha-particle confinement time. The total particle balance takes into account the admixture of helium ash and neon impurity. No helium is considered in the divertor region yet.

(c) The SOLPS4.3 code package is based on a combination of 2-dimensional fluid description of transport of the charged particles along and across the magnetic surfaces and a 3D Monte-Carlo model of neutral particle transport. The geometry of the problem is shown in Fig. 1. The two, top and bottom, divertors are symmetric and so is the double-null magnetic configuration. The component and reaction setup is similar to that in [8]. The plasma consists of ions and atoms of deuterium (representing both deuterium and tritium) and neon, as well as of D_2 molecules. No helium is presently considered in the model. Transport is flux-limited Spitzer-Harm along the magnetic field and anomalous across the magnetic surfaces. The values of the constant cross-field particle and heat diffusivities are adjusted [9] to reproduce the scrape-off layer (SOL) power width ~ 1.5 mm at the outer mid-plane, as follows from the experimental scaling [10]. Since we do not study helium removal here, there is no point in detailed modeling of the pumping conditions. We employ the "close box" model [11], where the density of the divertor plasma is characterized by the total particle (ions plus neutrals) content of deuterium and neon ions – respectively, N_D and N_{Ne}. Deuterium and neon gas puffing at low rate from the outer midplane and weak pumping from the top and bottom are introduced for technical reasons in order to control N_D and N_{Ne}. In the divertor region the heat loss by ionization of neutrals $P_{d,neut}$, the radiation of the impurities of $P_{d,imp}$ and the removal of heat to the divertor plates and on the wall P_{div} are calculated: $P_{SOL} = P_{d,\mathrm{rad}} + P_{div}$, where $P_{d,rad} = P_{d,neut} + P_{d,imp}$ is the total radiation from the divertor volume. Under the assumption of 100% recycling on the wall and divertor targets, the balance of hydrogen

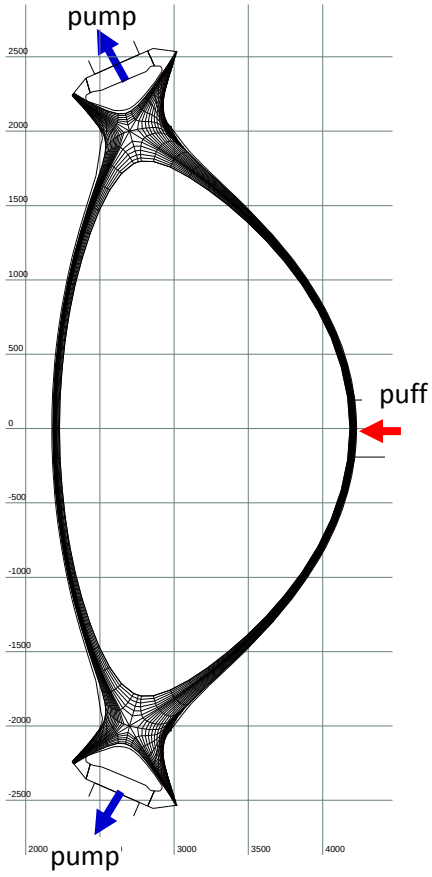

FIG.1 Geometry scheme and computational grid for DEMO-FNS divertor modeling.

particles in the divertor volume is written in the form: $p_n c_p = S_{puff} + S_{sep} - S_{0,sep}$, where c_p is the pumping rate, S_{puff} is the gas puffing source, which regulates the neutral pressure p_n.

(d) The integration of the main and divertor plasma models, in which the characteristic times of the main physical processes differ by orders of magnitude, is made within the framework of the approach proposed in [2]. In this approach, the results of simulation of divertor plasma are approximated by analytical dependences (scalings) between the fluxes of energy and particles coming out of the main plasma and gas puffing to the divertor plasma and the plasma parameters on the separatrix. These scalings are then used to set boundary conditions on the separatrix for the main plasma problem

(e) The neon density and radiation in the main plasma is calculated using the STRAHL code [12]. Impurity transport in the model is defined by the diffusion only, taken to be equal to the diffusion coefficient of main ions, so producing the uniform impurity profile determined by the boundary condition. No pinch and neoclassical effects are considered in the model.

(f) The plasma current is modeled as a result of solution of the poloidal flux of magnetic field diffusion equation with sources from the bootstrap current and the current drive by the neutral beam and neoclassical current conductivity. In a steady state the total plasma current is driven by currents from these sources.

(g) The penetration problem of fast beam atoms into the plasma is solved obtaining power density of ions and electrons heating profiles, the NB driven current density profile, the source of deuterium ions and the D-T fusion power from beam-plasma interaction. The beam is calculated using the NUBEAM code [13] taking into account charge-exchange, orbital and shine through losses. We use the deuterium beam with the atom energy of 500 keV.

(h) The pedestal on the temperature profiles of ions and electrons is set inside the separatrix according to scalings [14-15] for the value of pressure on the pedestal (beta poloidal) and for the width of the pedestal. For the ion density profile, the pedestal density value $n_{ped}=C\cdot\langle n_e\rangle$ is assumed to be proportional to the volume averaged electron density $\langle n_e\rangle$.

3. DIVERTOR MODELING RESULTS

The ultimate goal of divertor modeling reported here is producing scalings for the core-edge interface parameters of the plasma at the separatrix, which would allow formulating the boundary conditions for the core model. The physical properties of divertor plasmas are largely controlled by three principal parameters that determine the power level and the particle content of the working gas and radiating impurity [11]. The power input to the SOL, P_{SOL}, which is equal to the power loss with plasma particles from the core, is the obvious quantity to characterize the power level. For the particle content, the most natural choice, from the physical viewpoint, is the total numbers of nuclei of D and Ne in the computational domain outside the separatrix. However, this quantity is not easy to measure in experiment and not very convenient for integration with the core. Therefore, although our calculations are organized in terms of P_{SOL}, N_D and N_{Ne}, the final results will be presented in terms of P_{SOL}, the average neutral pressure near the pumping slots in the inner and outer divertor p_n and relative concentration of neon at the separatrix $c_{Ne} = \Sigma n_{Ne}/n_e$.

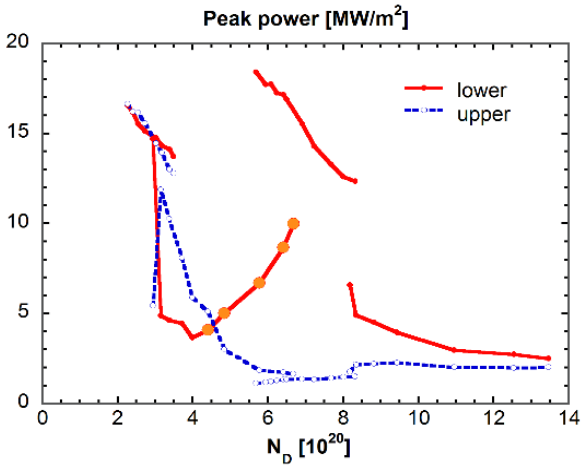

FIG. 2. Peak power loading of the lower and upper divertor targets vs. N_D. P_{SOL} = 30 MW, N_{Ne} = 10^{19}

We follow the procedure developed in [2] and following papers, organizing the code runs in series by varying N_D and keeping P_{SOL} and N_{Ne} constant inside each series. For a single-null divertor configuration, this approach resulted in mostly monotonic dependences that were convenient for approximation by a power type scaling [2]. However, this is not the case for a double-null configuration. Fig. 2 shows the dependence of the peak power loading of the upper and lower outer divertor targets on N_D. One can see that the solution of an up-down symmetric problem can be strongly asymmetric, with one of the divertors taking most of the power load. The physical nature of this symmetry break is related to the radiation-condensation instability [16]. If radiation dominates the power losses from the divertor plasma, then a perturbation of the plasma temperature T in the radiation zone can grow. Indeed, suppose that T slightly increases in one of the divertors. Then, in order to maintain the pressure balance along the magnetic field, the plasma density reduces correspondingly. If $P_{rad} \propto$

$n_e\, n_{Ne}\, L_R(T) = p_e\, p_{Ne}\, L_R(T)/T^2$, it can reduce by an increase of T, thus promoting further increase of the local temperature and reduction of the local density. Since transport along the magnetic field is much faster than across it, the density reduction in one of the divertors results in the density increase in the other one, thus provoking progressive cooling of the latter by the same mechanism.

Since this symmetry break causes a strong increase of the peak power loading of one of the targets, it should be avoided, and this imposes a new limitation on the control parameter values. Previously, for a single-null divertor, the density was limited by detachment [8] that correlates with deterioration of the core plasma confinement seen in experiment [17]. Now, in symmetric double-null, it becomes the symmetry break that limits the operational window of the divertor parameters before it gets limited by detachment. Having noticed that the asymmetry of the divertor loading can be in either direction, we rearrange the data into the "hot"-"cold", rather than "top"-"bottom" divertor and restrict the area of interest to that where the peak power loading of the targets is nearly symmetric. Such a procedure yields monotonic dependencies of the interface parameters, which allows reasonably good approximation of them by power functions. Following [8] we build the approximation of the type $u = A_u \mu^{B_u} P_{SOL}^{C_u} c_{Ne}^{D_u}$, where $u \in \{ q_{pk}, n_{e\_sep}, T_{e\_sep}, T_{i\_sep}, S_{0sep}, E_{0sep} \}$. μ is the neutral pressure normalized in such a way that $\mu = 1$ at the point of the symmetry break, $\mu = A_\mu p_n^{B_\mu} P_{SOL}^{C_\mu} c_{Ne}^{D_\mu}$. All the temperatures and neutral energy E_{0sep} are in eV, power in MW, q_{pk} in MW/m^2, n_e in 10^{20}m^{-3}, neutral flux S_{0sep} in 10^{20}s^{-1}, p_n in Pa. The approximation coefficients are given in the Table 1. Fig. 3 shows the result of application of this procedure for the peak power loading q_{pk}, the average electron density at the separatrix n_{e_sep} and the radiation fraction in the SOL and divertor $f_{rad} = P_{d,rad}/P_{SOL}$. One can see that, unlike the single-null ITER divertor case, (i) the separatrix density does not saturate with an increase of p_n (except for high neon density not compatible with good core performance) and (ii) the fraction of power radiated in the divertors does not exceed 50%.

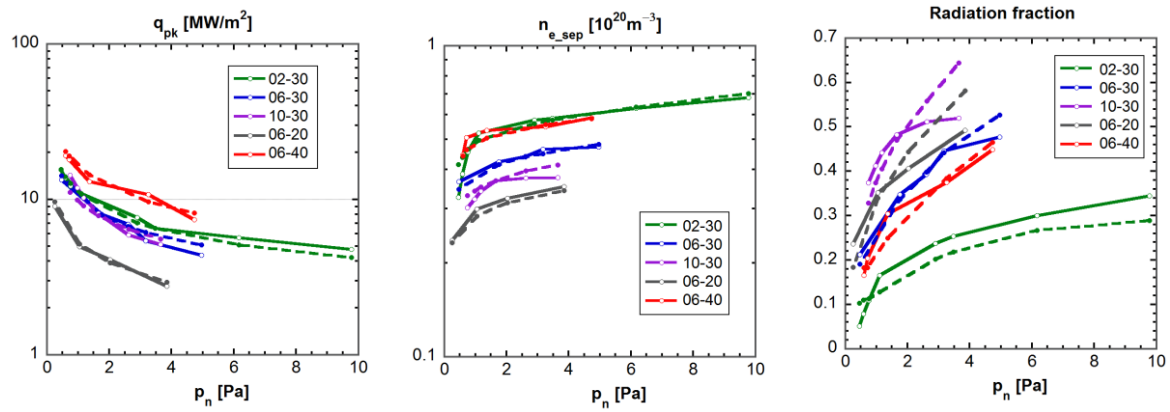

FIG. 3. The p_n dependence of q_{pk}, n_{e_sep} and f_{rad}. The line ends correspond to the up-down symmetry break. The dashed lines show the approximation quality (the approximation of f_{rad} is not important since this quantity does not appear in the boundary conditions for the core plasma). Different curves correspond to different neon level (total neon particle in the divertor region N_{Ne} =0.02-0.1·10^{20}) and power (P_{SOL}=20-40MW).

TABLE 1. APPROXIMATION COEFFICIENTS

	A	B	C	D
μ	1.37	1.102	-0.032	0.474
q_{pk}	0.044	-0.408	1.548	0.124
n_{e_sep}	0.023	0.099	0.628	-0.219
T_{e_sep}	75.5	-0.019	0.303	0.074
T_{i_sep}	223	-0.023	0.313	0.174
S_{0sep}	9.1	0.256	-0.046	-0.22
E_{0sep}	9.2	-0.018	0.666	-0.046

4 INTEGRATED MODELING RESULTS

We simulate the self-consistent problem to choose the optimal set of parameters for the neutron source with a maximum neutron yield not lower than G_{Neut}= 10^{19}s^{-1} and with a minimum peak thermal load on divertor targets not higher than q_{pk}= 10MW/m^2. Although the integrated modelling takes into account the large number of physical effects (a)-(h) the undefined parameters are there to be chosen. The set of these parameters is shown in the Table 2. It is useful to compare input parameters and calculation results with and without neon impurity. First of all we prescribe the energy confinement by the *H-factor*=1.3 underlining the essential sensitivity of fusion output to this parameter. Calculations show the decrease of the neutron yield from 1.4·10^{19}/s to 1·10^{19}/s with the reduction of *H-factor* to 1.1 value. By the way the energy confinement time decrease can be compensated by the increase of the additional power but we do not consider this path here. Another important parameter is the plasma electron density $<n_e>$ which determines the neutral beam penetration, bootstrap current and neutral beam current drive, fusion of both plasma –plasma and beam-plasma interaction, radiation power. The value of electron density has been chosen to satisfy all balances (a)-(h) and it is controlled by means of particle confinement coefficient c_p= τ_p/τ_E, and by the value of additional particle source S_{pel} that is taken to be the order of the separatrix neutral source S_{0sep}. The neon impurity density in the main plasma is controlled by the impurity source in the main plasma that determine the value of neon neutral density and the value of the total ion neon density Σn_{Ne} at the separatrix, as it is adjusted in the STRAHL code [12]. The relative neon density at the separatrix c_{Ne} in its turn is taken to be a parameter of the divertor model. In the case without impurity we prescribe 60% of P_{SOL} power to be radiated in the divertor region. Inclusion of neon impurity in the model allows to make this parameter defined. In the operation point chosen for DEMO-FNS c_{Ne} =0.02 and neon radiation provides 51% of the divertor power to be radiated. The tritium fraction f_T =0.7 is taken to maximaze the fusion output in case of D-beam [4] . It should be noted that in case of D-T-beam [5] maximization of fusion output occurs when the tritium fraction f_T =0.5. The helium accumulation in the main plasma is prescribed by the numerical coefficient c_{He}=4. It was obtained that the value of the density pedestal $n_{ped}/<n>$ has a little effect on the fusion output and the helium accumulation is negligibly low – the relative volume averaged helium density in the main plasma $<n_{He}>/<n_e>$ is about~ 0.4%.

Calculation results for chosen operational point for DEMO-FNS are shown in Tables 3-5 for two cases without and with neon impurity. First of all in order to fulfill the plasma current balance the averaged electron density $<n_e>$ was taken to be lower for the neon case. This also allowed to maintain the bremsstrahlung main ions and neon radiation P_{rad} on the reasonable level and keep the high ion temperature – it become even higher than the electron one. As a result the fusion power P_{DT} and neutron yield G_{Neut} become larger, fusion output from plasma-plasma and beam-plasma interaction kept the same contribution approximately the half power ratio. The peak power load on the divertor targets q_{pk} and value of μ in the neon case are kept on the reasonable level although the neutral pressure p_n was increased up to 4 Pa.

TABLE 2. UNDEFINED MODEL PARAMETERS

	H-factor	c_p	S_{pel}	S_{imp}	$P_{d,rad}/P_{SOL}$	f_T	c_{He}	$n_{ped}/<n>$
No impurity	1.3	3.8	185*10^{19}/c	-	60%	0.7	4	0.63
Neon impurity	1.3	2.9	217*10^{19}/c	2.1*10^{19}/c	51%	0.7	4	0.72

TABLE 3. SEPARATRIX AND DIVERTOR REGION PARAMETERS

	P_{SOL} MW	p_n Pa	μ	$T_{e,sep}$ keV	$T_{i,sep}$ keV	$n_{e,sep}$ 10^{19}m^{-3}	S_{0sep} 10^{19}s^{-1}	q_{pk} MW/m^2	c_{Ne}
No impurity	16.4	1	0.09	0.124	0.231	3.37	157	4.7	-
Neon impurity	36.5	4	0.88	0.169	0.349	5.12	176	7.5	0.02

TABLE 4. POWER, PARTICLE AND PLASMA CURRENT BALANCES

	τ_E	P_{rad}	S_{tot}	$<n_e>$	$T_e(0)$	$T_i(0)$	I_{pl}	I_{BS}	I_{CD}
	s	MW	10^{19}/s	10^{20}/m^3	keV	keV	MA	MA	MA
No impurity	0.77	2.4	355	1	11	9.8	4.3	2.2	2.1
Neon impurity	0.81	4.5	379	0.69	14.5	14.6	4.5	1.9	2.6

TABLE 5. FUSION PARAMETERS

	P_{DT} MW	G_{Neut} 10^{19}/s	P_{DT_pp} MW	P_{DT_bp} MW
No impurity	38.5	1.37	19.6	18.9
Neon impurity	39.9	1.42	18.5	21.4

In our calculations the level of neon density was varied and the scan results are shown in Fig. 4. It is seen from this figure that the increase or decrease of the value of c_{Ne} causes the plasma parameters to go outside the permissible range. In the regime with the high impurity level parameter μ become larger than one that would cause the up-down symmetry break as it was noted above. From the other side the low impurity level does not provide enough radiation to keep the peak power load on the admissible level q_{pk} < 10MW/m^2.

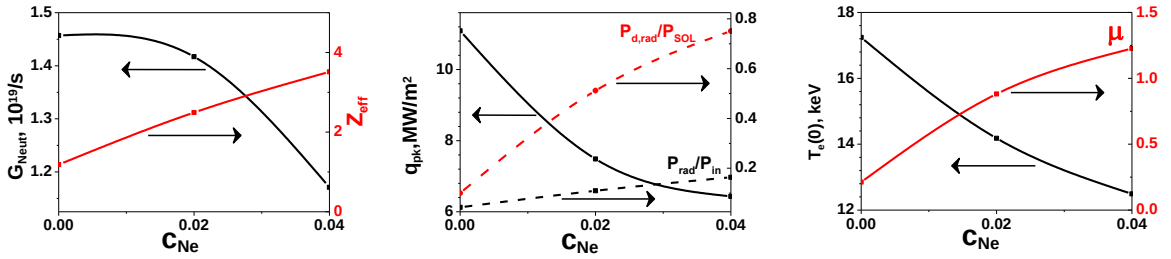

FIG.4 Relative impurity content $c_{Ne} = \Sigma n_{Ne}/n_e$ at the separatrix dependence of the total neutron yield G_{Neut}, volume averaged value of Z_{eff} in the main plasma, peak power load to the divertor targets q_{pk}, radiation fraction at the main plasma P_{rad}/P_{in}, and in the divertor zone $P_{d,rad}/P_{SOL}$, central electron temperature $T_e(0)$, and value of μ, determined in text.

5. CONCLUSIONS

The DEMO-FNS core transport modelling was carried out consistently with the divertor constraints. In the case of symmetric double-null divertor configuration, the achievable divertor plasma density can be limited by the spontaneous break of the up-down symmetry, which leads to high power loading of one of the targets. This effect limits also the achievable fraction of the radiation power in the divertors, hence reducing the divertor operational window in the parameter space. The second important point of the divertor task is the absence of saturation of n_{e_sep} by the density increase, which makes the density control in the core and edge interdependent and so more difficult in a machine significantly smaller than ITER.

The optimum operating point for DEMO-FNS steady-state regime is found using the integrated modelling and results are presented in Tables 2-5. The admissible parameter range is mostly defined by the energy confinement time and the impurity level. As for increasing the neon relative density c_{Ne} above the operation value 0.02 the peak power load decreases with the decrease of the fusion output. To the other side the decrease of the neon level cause the rise of the peak power load above permissible values. The decrease of the confinement parameter *H-factor* results fast in the drop of the fusion output. Also the plasma density, as a separate independent parameter, is important. It determines the neutral beam penetration, plasma current balance, fusion of both plasma –plasma and beam-plasma interaction, radiation power. Thus the rise of the plasma density could violate the plasma current balance that results in the decrease of the confinement time.

ACKNOWLEDGEMENTS

The work was partially supported by the State Atomic Energy Corporation ROSATOM

REFERENCES

[1] B.V. KUTEEV, YU.S. SHPANSKIY, and DEMO-FNS Team, Status of DEMO-FNS development, Nucl. Fus. **57** (2017) 076039

[2] G.W. PACHER, H.D. PACHER, A.S.KUKUSHKIN, G.JANESCHITZ, G.PEREVERZEV, Core plasma operation consistent with SOL parameters in ITER, J. Nucl. Mater., **313** (2003) 657

[3] C.GUILLEMAUT R.A.PITTS A.S.KUKUSHKIN M.O'MULLANE Radiative power loading in the ITER divertor, Fusion Eng. Des. **86** (2011) 2954

[4] YU.S. SHPANSKIY, and DEMO-FNS Team, "Progress in design of DEMO-FNS hybrid facility", *this conference*, IAEA-CN-258 FIP/P7-7 (2018)

[5] A.YU. DNESTROVSKIJ, B.V. KUTEEV, A.S. BYKOV, A.A. IVANOV, V.E. LUKASH, S.YU. MEDVEDEV, V.YU. SERGEEV, D.YU. SYCHUGOV, R.R. KHAYRUTDINOV, "Integrated modelling of DEMO-FNS current ramp-up scenario and steady-state regime, Nucl. Fus. **55** (2015) 063007

[6] V.YU. SERGEEV, B.V. KUTEEV, A.S. BYKOV, A.A. GERVASH, D.A. GLAZUNOV, P.R. GONCHAROV, A.YU. DNESTROVSKIJ, R.R. KHAYRUTDINOV, A.V. KLISHCHENKO, V.E. LUKASH, I.V. MAZUL, P.A. MOLCHANOV, V.S. PETROV, V.A. ROZHANSKY, YU.S. SHPANSKIY, A.B. SIVAK, V.G. SKOKOV, A.V. SPITSYN Conceptual design of divertor and first wall for DEMO-FNS, Nucl. Fus. **55** (2015) 123013

[7] G. V. PEREVERZEV, P.N. YUSHMANOV, "ASTRA. Automated System for Transport Analysis in a tokamak" Preprint Max-Planck-Institut fur Plasmaphysik ID 282186 (2002)

[8] H.D.PACHER, A.S.KUKUSHKIN, G.W.PACHER, V.KOTOV, R.A.PITTS, D.REITER, Impurity seeding in ITER DT plasmas in a carbon-free environment, J. Nucl. Mater. **463** (2015) 591

[9] A.S.KUKUSHKIN, H.D.PACHER, G.W.PACHER, V.KOTOV, R.A.PITTS, D.REITER, Consequences of a reduction of the upstream power SOL width in ITER, J. Nucl. Mater. **438** (2013) S203.

[10] T. EICH, A.W. LEONARD, R.A. PITTS, W. FUNDAMENSKI, R.J. GOLDSTON, T.K. GRAY, A. HERRMANN, A. KIRK, A. KALLENBACH, O. KARDAUN, A.S. KUKUSHKIN, B. LABOMBARD, R. MAINGI, M.A. MAKOWSKI, A. SCARABOSIO, B. SIEGLIN, J. TERRY, A. THORNTON, ASDEX Upgrade Team and JET EFDA Contributors, Scaling of the tokamak near the scrape-off layer H-mode power width and implications for ITER, Nucl. Fus. **53** (2013) 093031

[11] A. A. PSHENOV A. S. KUKUSHKIN, S. I. KRASHENINNIKOV, On detachment asymmetry and stability, Phys. Plasmas **24** (2017) 072508

[12] Dux R., "STRAHL user manual" *Technical Report No. IPP 10/30 IPP Max-Planck-Istitut für Plasmaphysik*, (2006).

[13] PANKIN A, MCCUNE D, ANDRE R, BATEMAN G, AND KRITZ A, The tokamak Monte Carlo fast ion module NUBEAM in the National Transport Code Collaboration library, Computer Physics Com. **159** (2004) 157-184

[14] P.B. SNYDER, R.J. GROEBNER, J.W. HUGHES, T.H. OSBORNE, M. BEURSKENS, A.W. LEONARD, H.R. WILSON, X.Q. XU, A first-principles predictive model of the pedestal height and width: development, testing and ITER optimization with the EPED model, Nucl. Fus. **51** (2011) 103016

[15] S.YU. MEDVEDEV, A.A. IVANOV, B.V. KUTEEV, V.E. LUKASH, R.R. KHAYRUTDINOV, MHD stability of ST-FNS [in Russian] Problems of Atomic Science and Technology, Series Thermonuclear Fusion **35** N2,(2012) 21

[16] A. S. KUKUSHKIN, S. I. KRASHENINNIKOV, submitted to Plasma Phys. Contr. Fusion (2018).

[17] A.HUBER, S.BREZINSEK, M.GROTH, P.C.DE VRIES, V.RICCARDO, G.VAN ROOIJ, G.SERGIENKO, G.ARNOUX, A.BOBOC, P.BILKOVA, G.CALABRO, M.CLEVER, J.W.COENEN, M.N.A.BEURSKENS, T.EICH, S.JACHMICH, M.LEHNEN, E.LERCHE, S.MARSEN, G.F.MATTHEWS, K.MCCORMICK, A.G.MEIGS, PH.MERTENS, V.PHILIPPS, J.RAPP, U.SAMM, M.STAMP, M.WISCHMEIER, S.WIESEN, JET-EFDA contributors, Impact of the ITER-like wall on divertor detachment and on the density limit in the JET tokamak JNM JNM, J. Nucl. Mater. **438** (2013) S139